PCCP

Atomic-scale models of early-stage alkali depletion and SiO_2-rich gel formation in bioactive glasses

Journal:	*Physical Chemistry Chemical Physics*
Manuscript ID:	CP-ART-10-2014-004711.R1
Article Type:	Paper
Date Submitted by the Author:	01-Dec-2014
Complete List of Authors:	Tilocca, Antonio; University College London, Chemistry

Journal Name

RSCPublishing

ARTICLE

Atomic-scale models of early-stage alkali depletion and SiO_2-rich gel formation in bioactive glasses

Cite this: DOI: 10.1039/xoxxoooooox

Antonio Tilocca[a]

Received ooth January 2012,
Accepted ooth January 2012

DOI: 10.1039/xoxxoooooox

www.rsc.org/

Molecular Dynamics simulations of Na^+/H^+-exchanged 45S5 Bioglass® models reveal that a large fraction of the hydroxyl groups introduced in the proton-exchanged, hydrated glass structure do not initially form covalent bonds with Si and P network formers but remain free and stabilised by modifier metal cations, whereas substantial Si-OH and P-OH bonding is observed only at higher Na^+/H^+ exchange levels. The strong affinity between free OH groups and modifier cations in the highly fragmented 45S5 glass structure appears to represent the main driving force for this effect. This suggests an alternative direct route for the formation of a repolymerised silica-rich gel in the early stages of the bioactive mechanism, not considered before, which does not require sequential repeated breaking of Si-O-Si bonds and silanol condensations.

Introduction

The interaction of a bioactive glass substrate with an aqueous medium is of central importance in all applications of these materials in biomedicine.[1, 2] The aqueous corrosion of the glass network eventually enables the release in the surrounding environment of soluble species such as calcium, silicate and phosphate, which have an established role in the bone-bonding and tissue-regenerating properties of the glass.[3, 4] In particular, the deposition of a calcium phosphate bone-like apatite layer that enables chemical bonding between living tissues and the glass substrate is enhanced by higher local concentrations of Ca and PO_4 species, with the silica species also involved in this process as nucleation sites.[5] Moreover, the special tissue-regeneration ability of some bioglasses such as 45S5 has been linked to the activation of osteogenic cells triggered by critical amounts of these same soluble calcium, silicate and phosphate species released from the glass matrix.[6]

Because the dissolution behaviour clearly reflects specific structural features of the glass such as bonding environments, network connectivity and ion clustering,[1] many investigations have focused on the bulk structure of the glass, and provided valuable information on the correlation between glass composition, structure, and bioactivity.[7-14] These studies can be considered *indirect* probes of the glass behaviour, because they aim to interpret and predict the glass dissolution and biological activity based on structural features measured for pristine dry compositions, either by experimental or modelling techniques.

More direct probes, for instance characterising the glass behaviour when the material is set in contact with an aqueous environment, are needed to support and extend the conclusions of the indirect studies above. The mechanism by which water interacts with the glass matrix is a key aspect that is starting to be elucidated. Ab-initio computer simulations have explored the interaction of molecular water with the glass surface and the bulk,[15-18] providing important insight on the most active surface adsorption sites, as well as on the state of a water molecule penetrating the glass matrix. This detailed information can now support a thorough exploration of the effect of hydration on a bioactive glass.

Following contact of soda-lime phosphosilicate bioglass like 45S5 with an aqueous biological medium, a rapid exchange of alkali (mainly sodium) ions from the glass with protons from the contact fluid is observed, followed by the formation of a silica-rich layer as sodium is leached and the alkali content of the glass is depleted.[19-26] The proposed mechanism accounting for these experimental observations generally involves rupture of Si-O-Si bridging bonds, formation of Si-OH silanols, and repolymerisation of adjacent Si-OH groups into Si-O-Si links to give a Si-enriched and Na-depleted gel layer.[3] However, a detailed description of the actual structural changes occurring in these early stages has not been obtained before, partly due to the difficulty to apply standard experimental techniques for characterising the rapid transformations occurring in the glass.[27] The formed SiO_2-rich gel layer plays a key role in protecting the glass against further corrosion,[28] while at the same time allowing migration and release of calcium and phosphate from the glass into the surrounding medium.[4, 29] A direct, atomic-scale investigation of the structure and formation of the silica-rich, alkali-depleted system starting from the pristine glass

would represent an important step forward in the current efforts towards rationalising the way in which these biomaterials work.[30] This goal is targeted here by obtaining relatively large models of ion-exchanged hydroxylated bioactive glass, which enable the exploration of the effect of gradual Na^+/H^+ exchange on the structural features of the alkali-depleted glass. The analysis allows us to draw a high-resolution description of the specific structural changes induced by this stage, and the ensuing formation of a silica-rich structure. Besides revealing a possible alternative mechanism for the silica-rich gel formation, the present results represents a substantial progress in our understanding of how the elementary interaction with water steers the behaviour of these biomaterials.

Methods

Systems of atomic composition $Na_{0.49-z}$ $Ca_{0.27}$ $P_{0.05}$ $Si_{0.46}$ $O_{1.56-z}$ $(OH)_z$, with z=0, 0.1, 0.3, and 0.49 were examined. z=0 corresponds to the base 45S5 composition, 46.1 SiO_2 24.4 Na_2O 26.9 CaO 2.6 P_2O_5, (mol%), and the corresponding model was taken from ref. [31]. The NaO→OH replacement for z>0 is obviously equivalent to a formal Na/H ion exchange: essentially, we model the gradual release of all sodium content from the glass by introducing OH^- units replacing NaO^- in the base dry composition. Rather than attempting to arbitrarily guess the sites and atoms of a stable structure that would be involved in and subjected to such exchange, each model is obtained by relaxing a fully random configuration containing specific OH amounts corresponding to the above compositions. This represents a more effective and unbiased way to determine the most stable exchanged structure without any arbitrary a priori assumption on the exchange process itself.

The hydrated glass models were obtained through classical Molecular Dynamics (MD) simulations using the DLPOLY program.[32] The present force field (Table S1 in the ESI) combines a shell-model (SM) potential developed[33] and successfully applied to model dry bioactive silicate glasses,[9, 14, 31, 34, 35] with additional terms describing hydroxyl groups and their interactions with the other ionic species in the glass. Each oxygen ion (i.e., non-hydroxyl O and hydroxyl Oh) is represented as a core-shell unit controlled by a harmonic spring. The Baram-Parker potential is used to represent OH groups as a core-shell oxygen (Oh_C-Oh_S) bonded to a proton via an Oh_S-H Morse potential.[36] In addition to Coulomb interactions between all ions and core-shell harmonic forces acting on each oxygen, Buckingham terms describe van der Waals interactions between all oxygen shells (O_S and Oh_S) and between oxygen shells and cations (M = Si^{4+}, P^{5+}, Na^+, Ca^{2+}). The additional Buckingham parameters for the M-Oh_S interactions were generally obtained by refitting the existing M-O_S ones through the auxiliary charges approach[37] to take into account the different ionic charge of O and Oh (Table S1). Finally, truncated three-body terms control O-Si-O and O-P-O angles. This combination of shell-model and hydroxyl potentials has proven accurate in a large number of computational studies of hydrated silicates, phosphates and other oxides.[38-42] Our previous study[43] confirmed that the same underlying SM force field for dry amorphous and crystalline silicates can be effectively integrated with the OH potentials above and with additional M-OH terms, derived from established M-O ones through the auxiliary charges approach, to incorporate different cationic species.

All MD simulations were carried out in the NVT ensemble, using damped adiabatic[44] core-shell dynamics with a 0.2 fs timestep, and a Berendsen thermostat to control the temperature. A similar procedure to that previously employed to model hydroxylated calcium silicate[45] and aluminosilicate[43] glasses was also followed for the compositions investigated here, although the procedure and purpose of OH incorporation are different in the present case. The approach involves heating and thermal annealing at 600-900 K of an initial random configuration of ~3000 atoms in the appropriate composition containing the required OH fraction, inserted in a cubic box of ~33 Å. The purpose of the high-temperature stage is simply to allow the system to efficiently explore the configurational space, rapidly removing unstable interactions, as assessed through the convergence of the configurational energy, which was relatively fast (between 1.5 and $3 \cdot 10^5$ timesteps). After the relaxation, a final constant-temperature run of 400 ps at 300 K was used first to equilibrate the system at room temperature and, after discarding the initial equilibration part, to produce the MD trajectory from which structural data were extracted and analysed. All data were averaged over two independent samples, started from different random configurations.

Results and Discussion

Figure 1 shows a snapshot extracted from the MD trajectory of the z=0.5 glass, illustrating how the OH groups (OHs) perturb the base 45S5 structure. While OHs bonded to network formers such as Si are clearly visible, at the same time a significant number of "free" OH groups, that is, bonded to neither Si or P, but coordinated to adjacent modifier cations (only Ca in the figure as the z=0.5 composition contains no sodium) are also present. In the following, these coordination modes and their effect on the glass structure are discussed more quantitatively, through statistical analysis of the MD trajectories.

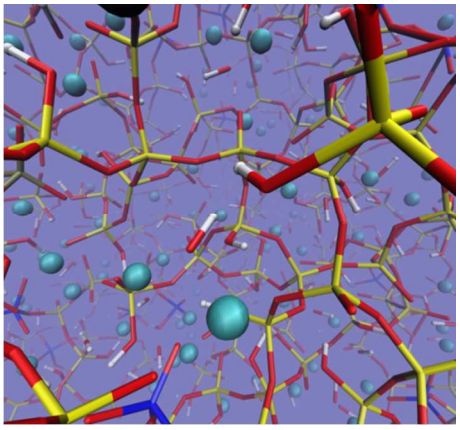

Figure 1: Structure of the z=0.5 glass composition. Si, P, Ca, O, and H atoms are coloured yellow, blue, cyan, red, and white, respectively.

OH coordination

Figure 2 illustrates the changes in the coordination shell of Si, P, Na, and Ca induced by gradual Na^+/H^+ exchange and increasing OH content. The left panel shows that both Si and P network formers remain tetracoordinated regardless of the OH content: the trends of OH and non-OH oxygen components of the overall coordination shell indicate that the unchanged coordination is achieved through an increasing bonded-OH component that matches the decreasing bonded-O fraction. In other words, the OH:O ratio within the coordination shell of Si and P changes as OH replaces O, but the total (OH+O) coordination number is unchanged. This trend appears more regular for Si, whereas there is no further increase in the fraction of OHs bonded to P above z=0.3.

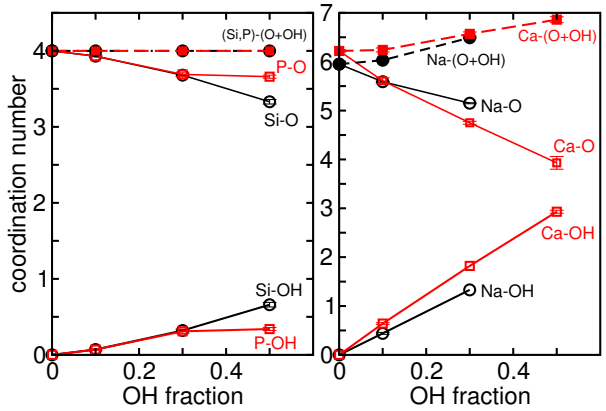

Figure 2: Oxygen coordination of silicon and phosphorus (left panel) and of sodium and calcium (right panel). Dashed lines in the top of the each panel connect the total (hydroxyl + non-hydroxyl, O+OH) coordination numbers, whose non-hydroxyl (O) and hydroxyl (OH) components are shown as solid lines.

The right panel of the figure highlights a somewhat different situation concerning the network modifiers Na and Ca. Whereas the number of OH and non-OH groups coordinated to a modifier ion respectively increase and decrease with the OH fraction, exactly as observed for the network formers, the total oxygen coordination of Na and Ca steadily increases, denoting an *expansion* in the oxygen coordination shell of both species with increasing OH content. This effect arises because the increasing OH component within the shell exceeds (rather than exactly match, as for Si and P) the decreasing non-OH component.

Table 1 characterises the distribution of hydroxyl groups through the corresponding fraction of OH bonded to Si, P, and to neither Si or P (the latter labelled "free OH"). A significant fraction of free OH groups is always present: these species are not bonded to a Si or P, but are strongly associated to the network modifiers, which balance their negative charge. The existence of these species in modified silicate glasses and melts is supported by experimental and ab-initio modelling evidences.[18, 46, 47] The free OHs are the dominant OH form at the lowest OH content; however, for higher contents, the Si-OH component increases at the expense of the free OH. As a consequence, the fraction of OH found in the Si coordination shell (Table 2) increases from 2 to 17%, while there is no further increase in the OH population of the P shell above z=0.3, mirroring the trend in Figure 2. The marked increase recorded in Table 2 also for the OH fraction occupying the coordination shells of Na and Ca (for z=0.5, almost 43% of the oxygen atoms coordinated to a calcium ion are hydroxyls) is not in contrast with the decreasing overall fraction of free OHs highlighted in Table 1: in fact, a free OH can be *shared* between network modifiers, in the sense that the same free OH can be found in the coordination shell of two or more Ca ions, for instance, and the extent of sharing will necessarily increase for higher OH contents.

Table 1: Percentage (with standard deviation in parentheses) of OH groups bonded to Si, to P, and to neither Si or P (free OH), in the proton-exchanged glasses

z(OH)	%OH-Si	%OH-P	%(free OH)
0.1	33 (1.0)	3.5 (0.5)	63.5 (1.5)
0.3	48.83 (0.8)	5.17 (0.5)	46.01 (0.3)
0.5	62.36 (2.6)	3.47 (0.2)	34.17 (2.4)

Table 2: OH fraction (standard deviation in parentheses) within the coordination shell of Si, P, Na, and Ca in the proton-exchanged glasses

z(OH)	$f(OH)^{Si}$	$f(OH)^{P}$	$f(OH)^{Na}$	$f(OH)^{Ca}$
0.1	1.79 (0.05)	1.75 (0.25)	7.33 (0.3)	10.2 (0.4)
0.3	7.96 (0.1)	7.75 (0.75)	20.55 (0.05)	27.74 (0.1)
0.5	16.61 (0.7)	8.5 (0.5)	-	42.76 (1.1)

The above trends can be graphically captured by highlighting the different kinds of OH (bonded to Si, P, or free) in the structure. Figure 3 illustrates the transition from a structure with predominance of free OH for z=0.1, to a structure with similar fractions of free and bonded OH (z=0.3), to a structure where the dominant OH type is that bonded to Si (z=0.5). This agrees with the indications of ab-initio simulations, that highlighted an intrinsically higher stability of "free" over bonded OH groups for very low water amounts dissolved in bulk bioglasses,[18] which further confirms the accuracy of the force field employed here. The observed trend may be interpreted as the free OH being the most stable state, which most OH can achieve at low OH concentration when sufficient metal cations are available to stabilize them. However, when the OH content is higher, the observed shift towards a predominantly OH-bonded distribution may reflect some kind of saturation of the modifier-rich sites that can host free OHs: in other words, OHs are first hosted in empty modifier-rich sites, but when these sites are filled and no longer available, additional OHs must form covalent bonds with silicon or phosphorus.

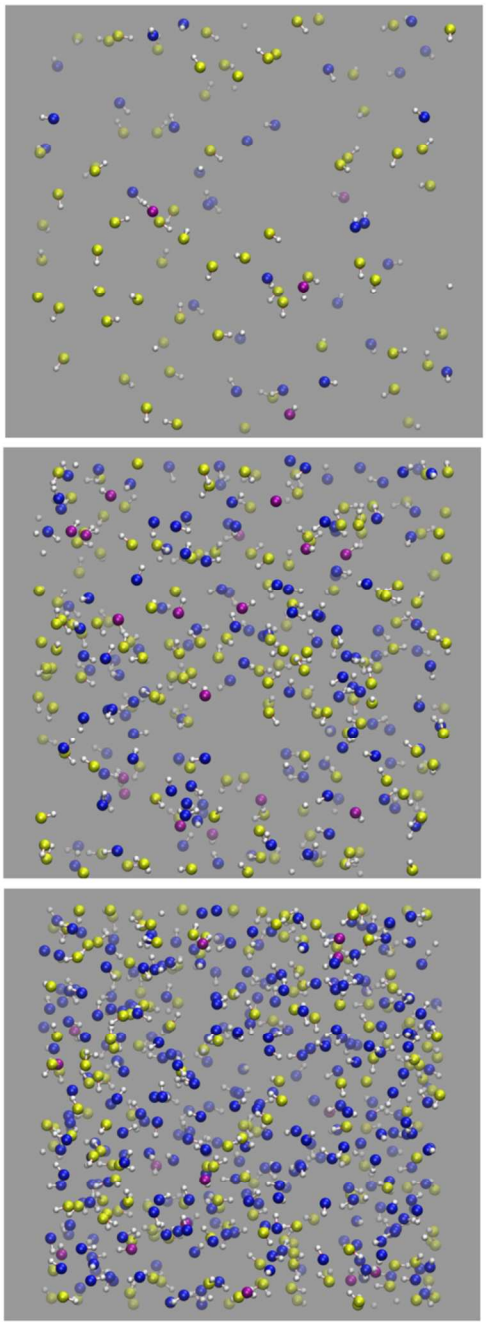

Figure 3: OH distribution across the Na^+/H^+-exchanged glass structures. Free, Si-bonded, and P-bonded OH groups are highlighted in yellow, blue and purple, respectively. Protons are coloured white. For clarity, Si, Na, Ca, P, and non-hydroxyl O atoms are not shown in the figure.

OH affinity for network modifiers and formers

The tendency of two species *m* and *n* to associate within the glass structure can be assessed through the ratios R_{mn} between the average number of species *n* found in the coordination sphere of *m* and those that would populate the same sphere if they were homogeneously distributed in all available volume.[8, 31, 48] In practice, R_{mn} is an unbiased measure of how close the arrangement of species *n* around *m* is to a uniform, homogeneous distribution: R_{mn}=1 denotes that there is neither mutual preference or avoidance between species *m* and *n*, whereas values higher (lower) than unity denote that the *n* species favour (avoid) *m* in their surroundings. An arrangement with species uniformly distributed in all available space, as in this approach, represents a more balanced reference to evaluate clustering properties compared to a fully random arrangement which is ultimately biased by the specific choice of distance constraints that must necessarily be applied to build it.

Figure 4 shows that, at low OH content (z=0.1), the region around a Si is depleted of OHs, as much as the region surrounding Na and – especially – Ca is enriched, compared to a homogeneous OH distribution. The OH population around Si gradually changes at intermediate and higher z contents, moving to uniform (R_{SiOH}=1.0±0.02 for z=0.3) to OH-enriched (R_{SiOH}=1.23±0.05 for z=0.5), with a concomitant opposite change in the association of OH with Na and Ca, denoted by R_{NaOH} and R_{CaOH} decreasing towards values typical of a more uniform distribution. These trends quantitatively confirm the effects noted above: free OHs attract modifier cations in their surroundings, while OHs eventually bond to Si and P at higher concentrations.

Complementary information comes from the R_{mm} factors concerning the interaction between two species of the same kind. Figure 4 shows that, while the Na-Na and Ca-Ca association remains approximately constant and unaffected by OH incorporation, OH-OH association changes from considerably to only slightly clustered with increasing OH content. Because, as inferred above, in diluted OH compositions OH groups preferentially associate with modifier ions, several OHs will be brought close to each other around a modifier in those conditions; however, as further modifier-OH aggregation becomes hindered for increasing OH content, for z=0.3-0.5 the overall OH association with modifiers and thus with each other is weakened.

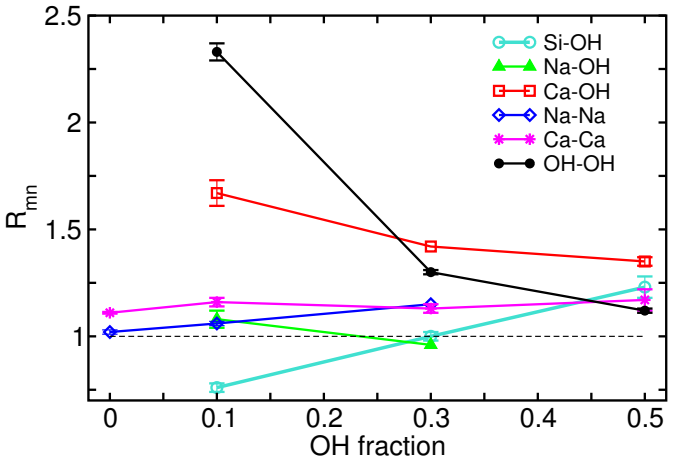

Figure 4: Calculated R_{mn} factors for different m-n pairs. The dashed horizontal line marks the R_{mn}=1 homogeneous condition.

Effect of Na/H exchange on the glass network connectivity

The impact of Na/H exchange on the glass network is illustrated in Figure 5, that shows the Q_n speciation of Si and P

(Q_n represents a Si or P atom bonded to *n* bridging oxygens, connecting it to *n* Si or P tetrahedra). Upon OH incorporation, the Si distribution (bottom panel) shifts towards higher-n species, with a decrease in the fraction of terminal (*n*=1) and chain (*n*=2) Q species and a corresponding increase in cross-linked (*n*=3 and 4) Si species. The P speciation, which is dominated by isolated (*n*=0) orthophosphates in the base composition, also shifts towards higher-n species for z>0. The Si and P network connectivities (NC)[49] (insets of Figure 5), defined as the average number of bridging oxygens (BOs) per Si or P, show a corresponding increase from 2.1 up to 2.6 for Si and from 0.2 up to 1.5 for P. The breakdown of the total NC in the corresponding Si-Si, Si-P, and P-P components highlights that the increases in NC(Si) and NC(P) reflect the formation of a higher number (relative to the z=0 case) of Si-O-Si and P-O-Si linkages, respectively, upon OH incorporation. An important aspect is that no OH groups bridging between two network formers are found: OHs are either terminal (bonded to a single Si or P), or free.

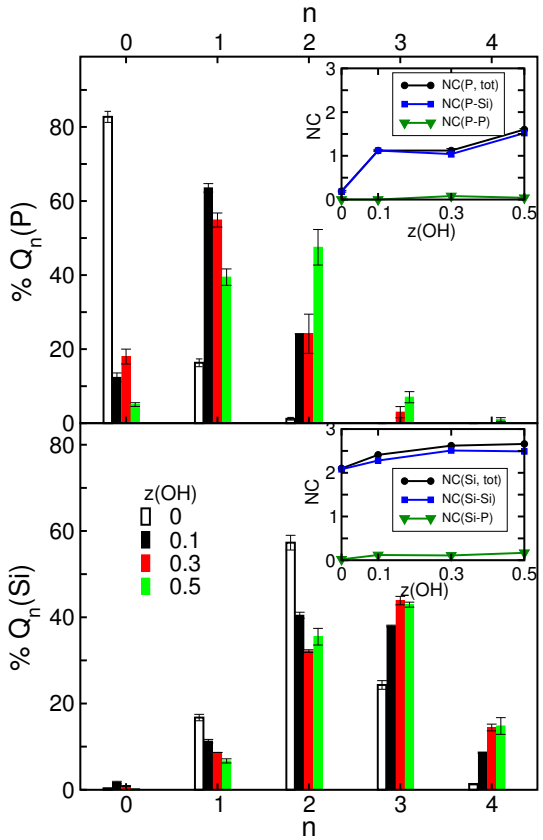

Figure 5. The Q_n distribution of Si (bottom) and P (top panel) for the dry (z(OH)=0) and hydroxylated (z(OH)=0.1-0.5) glasses. The inset of each panel shows the corresponding total and partial network connectivity.

Direct repolymerisation route

The NC increase upon Na^+/H^+ exchange suggests a direct route for the observed formation of a highly cross-linked silica-rich layer upon Na leaching, alternative or complementary to the proposed network repolymerisation by condensation of adjacent Si-OH groups. The direct route is made possible by the formation of a significant fraction of stable free OH groups, in addition to those bonded to Si or P. On the one hand, if the proton exchanged with Na^+ attaches to a non-bridging oxygen (NBO) bonded to a network former T, replacing the charge-balancing Na^+, as in $T–O^-Na^+ + H^+(aq) \rightarrow T–OH + Na^+(aq)$, no net change in the network connectivity of T will result. On the other hand, if a free OH group not bonded to T is formed, as in $T–O^-Na^+ + H^+(aq) \rightarrow T– + OH^- + Na^+(aq)$, the resulting "unsaturated" T– can form a new T–O–T' link bridging an available T'–O^- NBO, while the OH^- can coordinate another Na^+ or Ca^{2+} set free in the process, as in $T–O^-Na^+ + T'–O^-Ca^{2+} + H^+(aq) \rightarrow T–O–T' + Ca^{2+}OH^- + Na^+(aq)$ with a net NC increase owing to the conversion of a non-bridging to a bridging O. The latter process appears indeed possible because, as shown above, a free OH attracts Ca^{2+} ions, basically removing them from NBOs bonded to Si or P, and thus leading to repolymerisation of the phosphosilicate matrix. A similar analysis can be made considering the rupture of Na-balanced T–BO–T (rather than T–NBO) bonds upon Na^+/H^+ exchange. Therefore, the stability of free- and the instability of bridging-OH groups, highlighted by the analysis of the present models, suggest an alternative mechanism for silicate network repolymerisation, where the latter does not result from a sequence of Si-OH formation and condensation events, but can arise directly upon Na^+/H^+ exchange.

It can be argued whether or to what extent this effect of OH incorporation highlighted within a bulk environment can be representative of ion-exchange processes that start at the surface. Classical and ab-initio models have shown that the true surface region of a pristine 45S5 glass, with structural features markedly different from the bulk, involves the top ~ 5 Å, below which bulk-like structural environments are already recovered,[16, 50] and also showed that interfacial water can easily find pathways to penetrate within the highly fragmented 45S5 structure.[1] Therefore, the Na/H exchange processes often involve sites which are closer to bulk, in terms of structure and reactivity, than to surface sites. Moreover, OH groups formed upon the exchange can also rapidly find access to the inner, bulk-like regions, and thus their structural influence will primarily be expressed in a bulk-like environment. The investigation of OH groups arranged in a bulk rather than in a surface environment can thus be considered representative of the consequences of Na/H exchange on the structure of 45S5.

Conclusions

Following the initial Na^+/H^+ exchange, the formation of a silica-rich layer passivating the glass surface against further corrosion represents a key process for conventional bioactive glasses, because it allows the glass matrix to remain stable in the living environment long enough to support growth of new tissues, rather than rapidly dissolving.[4] Understanding how these processes are related and proceed is complicated by their rapid kinetics: for instance, the exact determination of the structure of the Si-rich layer itself is made difficult by the fast and often simultaneous deposition of calcium phosphates,

which complicate the analysis of diffraction and vibrational signals coming from it.[27] The clear evidence of alkali leaching and Si-rich layer formation[21-26] upon bioglass contact with a physiological fluid has led to developing models of these stages that involve OH^- directly attacking and breaking Si-O-Si links, and repolymerisation of the Si-OH groups formed in the first step.[3] However, explicit evidence of this mechanism for Si-rich layer formation is difficult to obtain: whereas there is no doubt that the silica-rich gel may proceed at least in part through the repeated breaking and condensation of Si-O-Si and Si-OH bonds, alternative or complementary routes for silica-rich gel formation that do not require Si-O-Si bond breaking cannot be ruled out. As a matter of fact, recent ab-initio calculations show that the most stable state for a water molecule dissolved in 45S5 Bioglass® is a dissociated state involving no broken Si–O bonds and a free hydroxyl.[18] The observed increase in Si–BO–Si concentration during leaching[3, 20] proves the formation of a repolymerised Si-rich matrix, but still does not fully clarify *how* this is achieved. The present simulations show that a repolymerised (higher-connectivity) phosphosilicate network can be directly formed upon Na^+/H^+ exchange when some of the OH groups associate with modifier cations rather than bond to Si, leading Si atoms to form bridging links with other Si in order to satisfy their oxygen coordination. Therefore, a network repolymerisation mechanism alternative to the one generally proposed for Si-rich layer formation in bioglasses appears possible based on the present simulations, in which new Si–O–Si bridges do not arise from condensation of Si–OH groups, but from OH-induced Si–O^-…Si cross-linking. The key to this mechanism, which determines its relative importance with respect to the alternative, is the formation of free, not-bonded OH groups stabilized by metal cations. The present results show that the free-OH mechanism is more likely at low Na^+/H^+ exchange levels, so that one may envisage a gradual transition between the two mechanisms as Na leaching proceeds and the silica-rich gel layer is progressively formed.

Acknowledgements

The author gratefully acknowledges the UK's Royal Society for financial support (RS-URF).

Notes and references

[a] Department of Chemistry, University College London, 20 Gordon Street, London WC1H 0AJ, U.K.

† Electronic Supplementary Information (ESI) available: force field parameters. See DOI: 10.1039/b000000x/

1. A. Tilocca, *J. Mater. Chem.*, 2010, **20**, 6848.
2. A. Hoppe, N. S. Güldal and A. R. Boccaccini, *Biomaterials*, 2011, **32**, 2757-2774.
3. J. R. Jones, *Acta Biomater.*, 2013, **9**, 4457-4486.
4. L. L. Hench, *J. Am. Ceram. Soc.*, 1998, **81**, 1705-1728.
5. M. M. Pereira, A. E. Clark and L. L. Hench, *J. Biomed. Mater. Res.*, 1994, **28**, 693-698.
6. L. L. Hench and J. M. Polak, *Science*, 2002, **295**, 1014-1017.
7. J. M. Smith, R. A. Martin, G. J. Cuello and R. J. Newport, *J. Mater. Chem. B*, 2013, **1**, 1296-1303.
8. Y. Xiang and J. Du, *Chem. Mater.*, 2011, **23**, 2703-2717.
9. G. Malavasi, A. Pedone and M. C. Menziani, *J. Phys. Chem. B*, 2013, **117**, 4142-4150.
10. J. K. Christie, J. Malik and A. Tilocca, *PCCP*, 2011, **13**, 17749-17755.
11. A. Tilocca and A. N. Cormack, *J. Phys. Chem. B*, 2007, **111**, 14256-14264.
12. H. Aguiar, E. L. Solla, J. Serra, P. González, B. León, F. Malz and C. Jäger, *J. Non-Cryst. Solids*, 2008, **354**, 5004-5008.
13. V. FitzGerald, D. M. Pickup, D. Greenspan, G. Sarkar, J. J. Fitzgerald, K. M. Wetherall, R. M. Moss, J. R. Jones and R. J. Newport, *Adv. Funct. Mater.*, 2007, **17**, 3746-3753.
14. A. Goel, S. Kapoor, A. Tilocca, R. R. Rajagopal and J. M. F. Ferreira, *J. Mater. Chem. B*, 2013, **1**, 3073-3082.
15. A. Tilocca and A. N. Cormack, *J. Phys. Chem. C*, 2008, **112**, 11936-11945.
16. A. Tilocca and A. N. Cormack, *ACS Appl. Mater. Interfaces*, 2009, **1**, 1324-1333.
17. A. Tilocca and A. N. Cormack, *Proc. R. Soc. A*, 2011, **467**, 2102-2111.
18. E. Berardo, M. Corno, A. N. Cormack, P. Ugliengo and A. Tilocca, *RSC Advances*, 2014, **4**, 36425-36436.
19. V. Banchet, E. Jallot, J. Michel, L. Wortham, D. Laurent-Maquin and G. Balossier, *Surf. Interface Anal.*, 2004, **36**, 658-665.
20. C. Y. Kim, A. E. Clark and L. L. Hench, *J. Non-Cryst. Solids*, 1989, **113**, 195-202.
21. A. E. Clark, C. G. Pantano and L. L. Hench, *J. Am. Ceram. Soc.*, 1976, **59**, 37-39.
22. M. Cerruti, C. L. Bianchi, F. Bonino, A. Damin, A. Perardi and C. Morterra, *J. Phys. Chem. B*, 2005, **109**, 14496-14505.
23. Y. Josset, F. Nasrallah, E. Jallot, M. Lorenzato, O. Dufour-Mallet, G. Balossier and D. Laurent-Maquin, *J. Biomed. Mater. Res.-A*, 2003, **67A**, 1205-1218.
24. H. Ylänen, K. H. Karlsson, A. Itälä and H. T. Aro, *J. Non-Cryst. Solids*, 2000, **275**, 107-115.
25. J. Mei, R. M. Shelton and P. M. Marques, *J. Mater. Sci.-Mater. M.*, 1995, **6**, 703-707.
26. C. R. Mariappan, D. M. Yunos, A. R. Boccaccini and B. Roling, *Acta Biomater.*, 2009, **5**, 1274-1283.
27. L. J. Skipper, F. E. Sowrey, D. M. Pickup, K. O. Drake, M. E. Smith, P. Saravanapavan, L. L. Hench and R. J. Newport, *J. Mater. Chem.*, 2005, **15**, 2369-2374.
28. D. M. Sanders and L. L. Hench, *J. Am. Ceram. Soc.*, 1973, **56**, 373-377.
29. A. Tilocca, *J. Chem. Phys.*, 2010, **133**, 014701-014710.
30. A. Tilocca, *PCCP*, 2014, **16**, 3874-3880.
31. A. Tilocca, *J. Chem. Phys.*, 2013, **139**, 114501.
32. http://www.ccp5.ac.uk/DL_POLY_CLASSIC.
33. A. Tilocca, N. H. de Leeuw and A. N. Cormack, *Phys. Rev. B*, 2006, **73**, 104209.
34. A. Tilocca, A. N. Cormack and N. H. de Leeuw, *Chem. Mater.*, 2007, **19**, 95-103.
35. A. Tilocca, *J. Mater. Chem.*, 2011, **21**, 12660-12667.
36. P. S. Baram and S. C. Parker, *Philos. Mag. B*, 1996, **73**, 49-58.
37. K. P. Schroder, J. Sauer, M. Leslie, C. R. A. Catlow and J. M. Thomas, *Chem. Phys. Lett.*, 1992, **188**, 320-325.
38. C. Chizallet and P. Raybaud, *Angew. Chem. Int. Ed.*, 2009, **48**, 2891-2893.
39. M. Zokaie, U. Olsbye, K. P. Lillerud and O. Swang, *J. Phys. Chem. C*, 2012, **116**, 7255-7259.
40. W. Gren, S. C. Parker, B. Slater and D. W. Lewis, *Journal of Physical Chemistry C*, 2010, **114**, 9739-9747.
41. D. Spagnoli, J. P. Allen and S. C. Parker, *Langmuir*, 2011, **27**, 1821-1829.
42. S. Kerisit, D. J. Cooke, D. Spagnoli and S. C. Parker, *J. Mater. Chem.*, 2005, **15**, 1454-1462.
43. J. Malik and A. Tilocca, *J. Phys. Chem. B*, 2013, **117**, 14518-14528.
44. P. J. Mitchell and D. Fincham, *J. Phys.-Condens. Mat.*, 1993, **5**, 1031-1038.
45. R. N. Mead and G. Mountjoy, *Chem. Mater.*, 2006, **18**, 3956-3964.
46. S. C. Kohn, R. Dupree and M. E. Smith, *Geochim. Cosmochim. Acta*, 1989, **53**, 2925-2935.
47. X. Xue and M. Kanzaki, *Geochim. Cosmochim. Acta*, 2004, **68**, 5027-5057.
48. R. N. Mead and G. Mountjoy, *J. Phys. Chem. B*, 2006, **110**, 14273-14278.

49. Z. Strnad, *Biomaterials*, 1992, **13**, 317-321.
50. A. Tilocca and A. N. Cormack, *Langmuir*, 2010, **26**, 545-551.

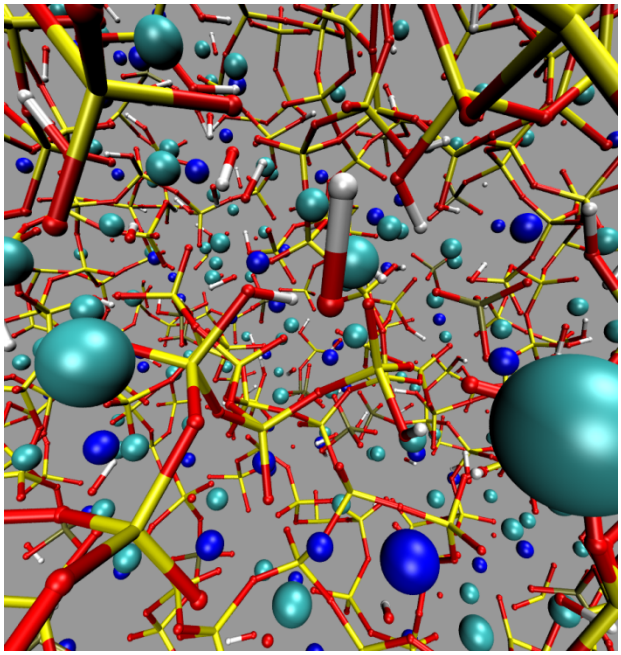

Molecular Dynamics simulations of Na^+/H^+-exchanged 45S5 Bioglass® reveal the co-existence of bonded and non-bonded hydroxyls, suggesting a direct mechanism for forming a silica-rich gel structure upon the initial ion exchange.